



**HAL**  
open science

# A Complete Model of a Two Degree of Freedom Platform Actuated by Three Pneumatic Muscles Elaborated for Control Synthesis

David Bou Saba, Eric Bideaux, Xavier Brun, Paolo Massioni

► **To cite this version:**

David Bou Saba, Eric Bideaux, Xavier Brun, Paolo Massioni. A Complete Model of a Two Degree of Freedom Platform Actuated by Three Pneumatic Muscles Elaborated for Control Synthesis. BATH/ASME 2016 Symposium on Fluid Power and Motion Control, Sep 2016, Bath, United Kingdom. 10.1115/FPMC2016-1706 . hal-01400091

**HAL Id: hal-01400091**

**<https://hal.science/hal-01400091>**

Submitted on 29 Mar 2023

**HAL** is a multi-disciplinary open access archive for the deposit and dissemination of scientific research documents, whether they are published or not. The documents may come from teaching and research institutions in France or abroad, or from public or private research centers.

L'archive ouverte pluridisciplinaire **HAL**, est destinée au dépôt et à la diffusion de documents scientifiques de niveau recherche, publiés ou non, émanant des établissements d'enseignement et de recherche français ou étrangers, des laboratoires publics ou privés.

# DRAFT: A COMPLETE MODEL OF A TWO DEGREE OF FREEDOM PLATFORM ACTUATED BY THREE PNEUMATIC MUSCLES ELABORATED FOR CONTROL SYNTHESIS

David Bou Saba, Eric Bideaux, Xavier Brun, Paolo Massioni

Ampere Laboratory  
Institut National des Sciences Appliquées de Lyon  
Université de Lyon  
Villeurbanne, 69621  
France

Email: david.bou-saba@insa-lyon.fr, eric.bideaux@insa-lyon.fr  
xavier.brun@insa-lyon.fr, paolo.massioni@insa-lyon.fr

## ABSTRACT

*Pneumatic muscles have a high potential in industrial use, as they provide safety, high power over volume ratio, low price and wide range of pulling effort. Nevertheless, their control is quite hard to achieve due to the non linearity and hysteresis phenomena, plus the uncertainties in their behavior. This paper presents the modeling of a two degree of freedom platform actuated by three pneumatic muscles for control purposes. Three servovalves are used to supply airflow inside the muscles. The innovative concept is the modeling of each component including the static and dynamic muscle behavior. The model of the servovalve consists of a look-up table gathering the three variables: airflow, pressure and voltage applied to the servovalve. In addition, a thermodynamic and a mechanical study of the system complete the model. The result is a complete model design having as input the voltage applied to the three servovalves, and as outputs, the two angles of rotation. Simulated and experimental results permit to validate the complete model for high variation in static and dynamic conditions. These results will be helpful for nonlinear control synthesis.*

## NOMENCLATURE

$\theta_0$  Weave angle of the muscle at rest  
 $D_0$  Diameter of the muscle at rest

$l_0$  Length of the muscle at rest  
 $\varepsilon_0$  Initial contraction of the muscle  
 $\alpha$  Experimentally determined power coefficient  
 $A$  Experimentally determined coefficient  
 $B_1$  Experimentally determined coefficient  
 $B_2$  Experimentally determined coefficient  
 $k$  Polytropic index of air (1.4)  
 $r$  Specific gas constant  
 $T$  Air temperature  
 $R$  Distance separating the center of the platform and the muscle application point  
 $J$  Platform moment of inertia about an horizontal axis  
 $\phi_1$  Angular position of the first muscle  
 $\phi_2$  Angular position of the second muscle  
 $\phi_3$  Angular position of the third muscle  
 $\theta_x$  Angular position of the platform about  $x$  axis  
 $\theta_y$  Angular position of the platform about  $y$  axis  
 $P$  Absolute pressure inside the muscle  
 $P_g$  Gauge pressure inside the muscle  
 $u$  Voltage applied to the servovalve  
 $V$  Volume of the muscle  
 $q$  Air flow  
 $\varepsilon$  Contraction of the muscle  
 $F$  Tension of the muscle  
 $\Gamma_f$  Friction torque due to the contact in the spherical joint

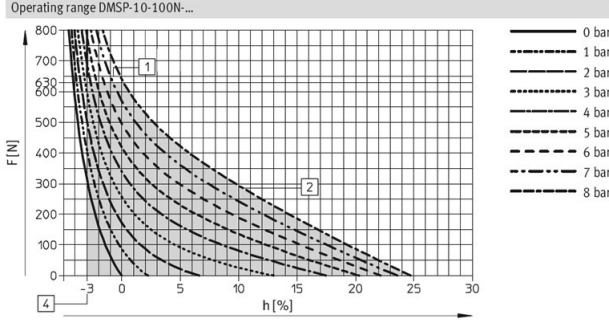


FIGURE 1. MUSCLE CHARACTERISTICS BY FESTO

## INTRODUCTION

Pneumatic muscles have been widely studied for many engineering and robotic applications, due to their high power over volume ratio, low price and high pulling efforts they can produce [4]. The difficulty of dealing with a pneumatic muscle arises from the non-linearity in its behavior (see Fig. 1) as well as from the hysteresis phenomena encountered in it. The effort produced by the muscle depends on both pressure and length contraction and has a high non linear evolution. Many theoretical models of the pneumatic muscle can be found in the literature [4–6]. However, the model we adopt is a result of experimental tests [1] that took the hysteresis phenomena into account and presented a more accurate behavior. In this article, we make the complete modeling of a platform based on three pneumatic muscles (see Fig. 3). Our objective is the synthesis of a model based control law that will allow us to achieve a trajectory tracking of the system in a wide operating range of the muscle. The platform is restrained to move in a certain operating domain due to physical constraints and to the fact that the muscles generate only pulling efforts. Furthermore, the system requires a control allocation strategy to solve the over-actuation. The latter results from having three control inputs and only two outputs.

A sliding mode controller combined with adaptive fuzzy CMAC was proposed in [2] for a parallel platform based on pneumatic muscles. The innovative control approach we take into consideration is the inverse model of the system and the resolution of the over-actuation of this platform.

The paper is structured as follows: first, we present the model of each component, starting with the kinematic and dynamic modeling of the platform, then the quasi-static and dynamic model of the muscle and the servovalve model. Experimental validation of the complete system is shown in a third part. A resolution of the over-actuation is proposed. Finally, the inverse model control is derived, and some experimental results of the system controlled using an input-output linearization approach are given.

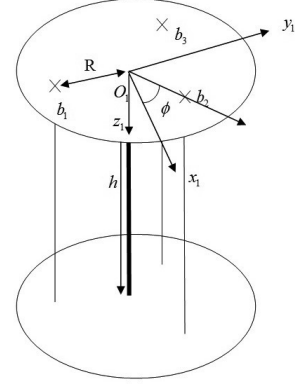


FIGURE 2. 3D SKETCH OF THE PLATFORM

## MODELING OF THE PLATFORM

The system we are studying consists of a moving platform, based on a central spherical joint and three pneumatic muscles, symmetrically disposed ( $120^\circ$  out of phase around the central axis). The twist rotation and the vertical displacement of the platform are constrained by placing a vertical link between the latter and the fixed base in the center and by imposing only vertical movement to the muscles. Thus, the platform has 2 degrees of freedom in rotation: the roll and pitch (see Fig. 2).

The assembly of the muscles is as follows: a pivot joint is implemented between each muscle and the fixed base, and a spherical joint between each muscle and the moving platform. We will denote by  $\phi_i$ ,  $i = 1 \dots 3$  the angular positions of the points  $b_i$  with respect to  $x_1$  axis, where  $b_i$  is the attachment point of the muscle to the platform in the reference frame  $R_1(O_1, x_1, y_1, z_1)$  linked to the platform as shown in Fig. 2.  $\phi_1 = -\frac{\pi}{2}$  rad for the first muscle,  $\phi_2 = \frac{\pi}{6}$  rad for the second muscle and  $\phi_3 = 5\frac{\pi}{6}$  rad for the third one.

The inclination of the platform is measured using an inclinometer placed at its center. Pressure values inside the muscles are measured by three pressure sensors, and the muscles are controlled by three servovalves. The assembly of the platform is represented in Fig. 3. Table 1 gives the values of some experimental parameters, while the characteristics of the inclinometer, the pressure sensor and the servovalve are given in Tab. 2.

## Kinematic Modeling

The rotation matrix from the reference frame  $R_1$  linked to the platform to the fixed horizontal basis  $R_0$  is:

$$R_{1 \rightarrow 0} = \begin{bmatrix} \cos \theta_y & \sin \theta_x \sin \theta_y & -\sin \theta_y \cos \theta_x \\ 0 & \cos \theta_x & \sin \theta_x \\ \sin \theta_y & -\sin \theta_x \cos \theta_y & \cos \theta_x \cos \theta_y \end{bmatrix} \quad (1)$$

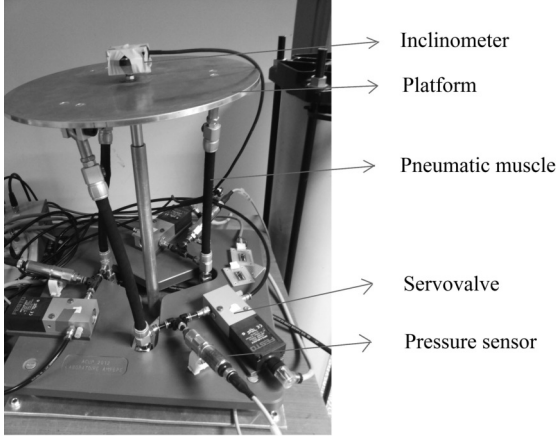


**FIGURE 3.** PLATFORM EXPERIMENTAL STRUCTURE

**TABLE 1.** EXPERIMENTAL DATA OF THE SYSTEM

Platform material	Aluminium	
Platform diameter	30	<i>cm</i>
Platform thickness	5	<i>mm</i>
$R$	0.1	<i>m</i>
$J$	0.0054	<i>kg.m<sup>2</sup></i>
$D_0$	0.01	<i>m</i>
$l_0$	0.2	<i>m</i>
$\theta_0$	0.3979	<i>rad</i>

The points  $b_i$  are assumed to only move in a vertical direction. Their displacements through  $z_1$  axis are obtained by multiplying their coordinate vectors by the third row of the matrix  $R_{1 \rightarrow 0}$ . Thus, the length contraction of each muscle can be written as:

$$\varepsilon_i = \frac{R}{l_{0i}} (\cos \phi_i \sin \theta_y - \sin \phi_i \sin \theta_x \cos \theta_y) + \varepsilon_{0i} \quad (2)$$

The contraction velocity of each muscle is the time derivative of  $\varepsilon_i$

$$\dot{\varepsilon}_i = \frac{R}{l_{0i}} \left[ -\dot{\theta}_x \sin \phi_i \cos \theta_x \cos \theta_y + \dot{\theta}_y (\cos \phi_i \cos \theta_y + \sin \phi_i \sin \theta_x \sin \theta_y) \right] \quad (3)$$

**TABLE 2.** INCLINOMETER AND PRESSURE SENSOR CHARACTERISTICS

Inclinometer		Characteristics	
Type	G-NSDOG2-001		
Resolution	12 bit		
Measuring range	$-90^\circ$	$+90^\circ$	
Uncertainty	0.15°		
Pressure sensor		Characteristics	
Type	SDET-22T-D10-G14-U-M12		
Output voltage range	0.1 - 10 V		
Measuring range	0 - 10 bar		

where the following assumptions are made:

$$\begin{cases} l_{0i} = l_0 & i = 1 \dots 3 \\ \varepsilon_{0i} = \varepsilon_0 & i = 1 \dots 3. \end{cases}$$

### Direct Dynamic Modeling

Considering the Lagrangian formalism [3], virtual work and generalized forces, the direct dynamic model of the platform can be derived, giving the expression of the angular accelerations in terms of the efforts exerted by the muscles on the platform.

$$\begin{bmatrix} \ddot{\theta}_x \\ \ddot{\theta}_y \end{bmatrix} = M(\theta_x, \theta_y) \begin{bmatrix} F_1 \\ F_2 \\ F_3 \end{bmatrix} - \frac{1}{J} \Gamma_f(\dot{\theta}_x, \dot{\theta}_y) \quad (4)$$

where the matrix  $M(\theta_x, \theta_y)$  is given in equation (5).

The friction term will not be modeled in this article. It will be considered as a disturbance.

### Quasi-Static Model Of The Muscle

The aim of the quasi-static model of the muscle is to represent the expressions of the traction force  $F$  and the muscle volume  $V$  as functions of the contraction  $\varepsilon$ , the gauge pressure inside the muscle and some of its intrinsic characteristics. Theoretical formulations can be found in [4–6]. In these articles, the muscle had been considered a lossless system with no energy storage, and by adopting the energy conservation approach, the virtual work argument yields to the theoretical expressions. However, the errors encountered in the theoretical modeling result

$$M(\theta_x, \theta_y) = \frac{R}{J} \begin{bmatrix} -\sin \phi_1 \cos \theta_x \cos \theta_y & -\sin \phi_2 \cos \theta_x \cos \theta_y & -\sin \phi_3 \cos \theta_x \cos \theta_y \\ \cos \phi_1 \cos \theta_y + \sin \phi_1 \sin \theta_x \sin \theta_y & \cos \phi_2 \cos \theta_y + \sin \phi_2 \sin \theta_x \sin \theta_y & \cos \phi_3 \cos \theta_y + \sin \phi_3 \sin \theta_x \sin \theta_y \end{bmatrix} \quad (5)$$

from considering the muscle as a continuous cylindrical shape, whereas the ends take a conical shape when contracted [6]. To overcome this side effect, a parameter that amplifies the correction ratio was introduced in [6], and an exponential function with two constants was suggested for this factor in [7]. In this article, we will refer to [1], where the evolution of  $F$  and  $V$  had been determined experimentally. Assuming a linear dependency on the pressure, the following form was suggested for the effort expression:

$$F(P_g, \varepsilon) = H(\varepsilon)P_g + L(\varepsilon), \quad (6)$$

where

$$L(\varepsilon) = A \frac{\varepsilon(\varepsilon - B_1)}{\varepsilon + B_2} \quad (7)$$

and

$$H(\varepsilon) = \frac{\pi D_0^2}{4} \left[ \frac{3(1-\varepsilon)^\alpha}{\tan^2 \theta_0} - \frac{1}{\sin^2 \theta_0} \right] \quad (8)$$

with  $\alpha > 2$ .

While the standard model considers only the first part of the right hand side of eq. (6) with  $\alpha = 2$ , a second term  $L(\varepsilon)$  (described in eq.(7)) had been added in order to model the material (elastomeric membrane) stiffness that contributes in the effort exerted and in the hysteresis phenomena. Besides, since  $L(\varepsilon)$  is independent of the pressure, it is then equal to the effort exerted by the muscle at zero gauge pressure.

Eq. (8) is quite similar to the theoretical expression, however, the exponent of  $(1 - \varepsilon)$  is taken as a parameter  $\alpha$  instead of 2. The parameters  $\alpha$ ,  $A$ ,  $B_1$  and  $B_2$  had been experimentally identified. Figures 4 and 5 show the matching of the experimental characteristics of the relationship  $(F, P, \varepsilon)$  [1] with the chosen model.

A compensation strategy for the hysteresis in the nonlinear force characteristic of pneumatic muscles is proposed in [1]. The method is to consider the mean effort curve of the two curves obtained in both inflating and deflating for each pressure for identification.

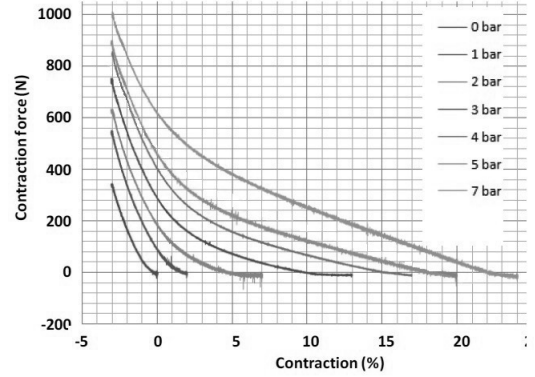


**FIGURE 4.** EXPERIMENTAL CHARACTERISTICS OF THE RELATIONSHIP  $(F, P, \varepsilon)$

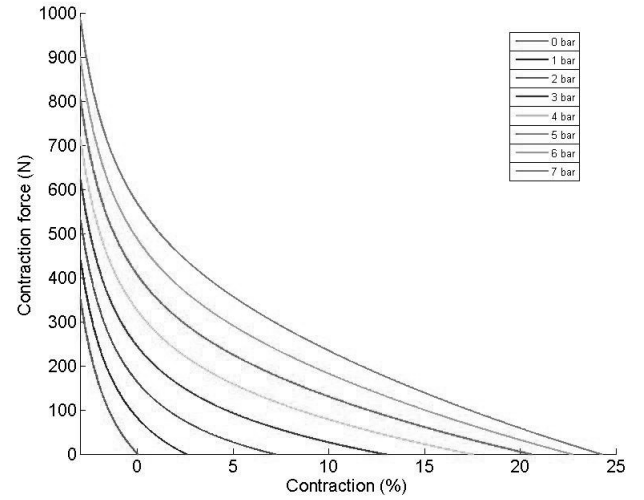


**FIGURE 5.** PLOTS OF THE EXPERIMENTALLY DETERMINED EXPRESSION OF THE QUASI-STATIC MODEL OF THE MUSCLE

An adjusted model of the volume can also be found in [1], where the rubber deformation influence on the volume had been taken into account. Furthermore, it has been shown that the volume of the muscle is nearly independent of the pressure in the air

chamber of the muscle, it is rather a function of the contraction. The experimentally found expression is written as follows

$$V(\varepsilon) = \frac{\pi}{4} D_0^2 l_0 \left[ \frac{1}{\sin^2 \theta_0} - \frac{(1-\varepsilon)^\alpha}{\tan^2 \theta_0} \right] (1-\varepsilon). \quad (9)$$

### Dynamic model Of The Muscle

In order to get the variation of the pressure as a function of the different variables, we assume the following: (i) the muscle can be considered as a variable volume chamber containing a compressible fluid (air), (ii) the thermodynamic variables (pressure, temperature and density) of the gas are uniform inside the muscle, (iii) the inlet and outlet flow is quasi-stationary (transient state negligible), (iv) a polytropic model of the gas behavior takes place in the chamber, (v) the height difference between pressurizing point and exhaust point is negligible and (vi) there is no air leakage through the muscle.

The pneumatic model can then be written as follows [1]

$$\frac{dP}{dt} = \frac{1}{1 + \frac{kP}{V(P,\varepsilon)} \frac{\partial V(P,\varepsilon)}{\partial P}} \left[ -\frac{kP}{V(P,\varepsilon)} \frac{\partial V(P,\varepsilon)}{\partial \varepsilon} \dot{\varepsilon} + \frac{krT}{V(P,\varepsilon)} q(P,u) \right] \quad (10)$$

Nevertheless, since the volume is related only to the contraction, i.e.  $\frac{\partial V(P,\varepsilon)}{\partial P} = 0$  [1], the thermodynamic model derived in equation (10) can therefore be reformulated as follows

$$\dot{P} = \frac{krT}{V(\varepsilon)} \left[ q(P,u) - \frac{P}{rT} \frac{\partial V(\varepsilon)}{\partial \varepsilon} \dot{\varepsilon} \right] \quad (11)$$

where

$$\frac{\partial V}{\partial \varepsilon}(\varepsilon) = \frac{\pi}{4} D_0^2 l_0 \left[ -\frac{1}{\sin^2 \theta_0} + (\alpha + 1) \frac{(1-\varepsilon)^\alpha}{\tan^2 \theta_0} \right]. \quad (12)$$

### Model Of The Servovalve

The main advantage of using a servovalve instead of an ON/OFF valve is the possibility of regulating the desired flow inside the muscle and thus the pressure in the air chamber by controlling the voltage applied to the servovalve. The servovalve we are using (type MPYE-5-M5-010-B) is globally modeled in [8], where the characterization is carried out by experimental measurements.

The flow depends on the voltage applied to the servovalve, the supply pressure, which is kept constant during the tests, the pressure inside the muscle and the exhaust pressure which is equal to the atmospheric pressure. The temperature during the tests is assumed to be constant (ambient temperature). The characterization of the servovalve is a 3D graph that represents the

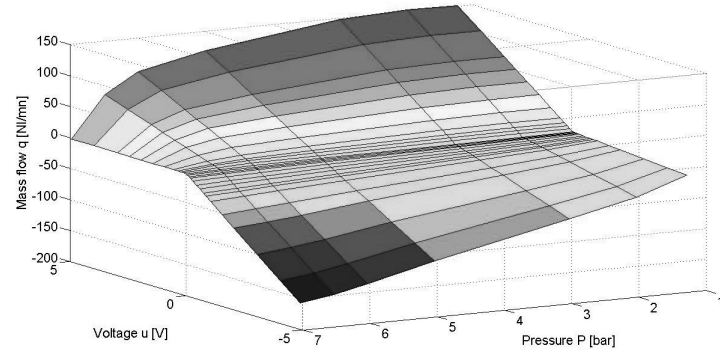


FIGURE 6. CHARACTERISTICS OF THE SERVOVALVE [8]

mass flow rate  $q$  evolution as function of the electrical input of the electronic stage  $u$  and the pressure  $P$  inside the muscle for a set supply and exhaust pressures (see Fig. 6).

The dynamic model of the servovalve is a second order transfer function, with a bandwidth of 100 Hz, and a damping coefficient equal to 1.

### COMPLETE MODEL SIMULATION AND EXPERIMENTAL VALIDATION

At least, seven state variables have to be considered in the system we described. The global model of the platform can be summarized as follows

$$\frac{d}{dt} \begin{bmatrix} \theta_x \\ \theta_y \end{bmatrix} = \begin{bmatrix} \dot{\theta}_x \\ \dot{\theta}_y \end{bmatrix} \quad (13)$$

$$\frac{d}{dt} \begin{bmatrix} \dot{\theta}_x \\ \dot{\theta}_y \end{bmatrix} = M(\theta_x, \theta_y) \begin{bmatrix} F_1 \\ F_2 \\ F_3 \end{bmatrix} - \frac{1}{J} \Gamma_f(\dot{\theta}_x, \dot{\theta}_y) \quad (14)$$

$$\frac{dP_i}{dt} = \frac{krT}{V(\varepsilon_i)} \left[ q(P_i, u_i) - \frac{P_i}{rT} \frac{\partial V(\varepsilon_i)}{\partial \varepsilon_i} \dot{\varepsilon}_i \right], \quad i = 1 \dots 3 \quad (15)$$

Using the different models presented above, we can build a Simulink scheme that simulates our system consisting of the platform, three pneumatic muscles and three servovalves. Figure 7 is a representation of this scheme. The inputs of the system are the voltage supplied to the servovalve, and the outputs are the two angles of rotation,  $\theta_x$  and  $\theta_y$ , of the platform. It is important to notice that the variables  $u$ ,  $q$ ,  $\dot{P}$ ,  $P$ ,  $F$ ,  $\varepsilon$ ,  $\dot{\varepsilon}$  are three dimensional vectors, whereas  $\theta$ ,  $\dot{\theta}$ ,  $\ddot{\theta}$  are two dimensional vectors.

Figures 8, 9 and 10 show the response of the platform, i.e. the two angles  $\theta_x$  and  $\theta_y$ , and the pressure evolution of the muscle 3, in both simulation and experimentation. The input is a ramp in  $u_1$  applied to muscle 1, followed by a ramp in  $u_2$  applied to

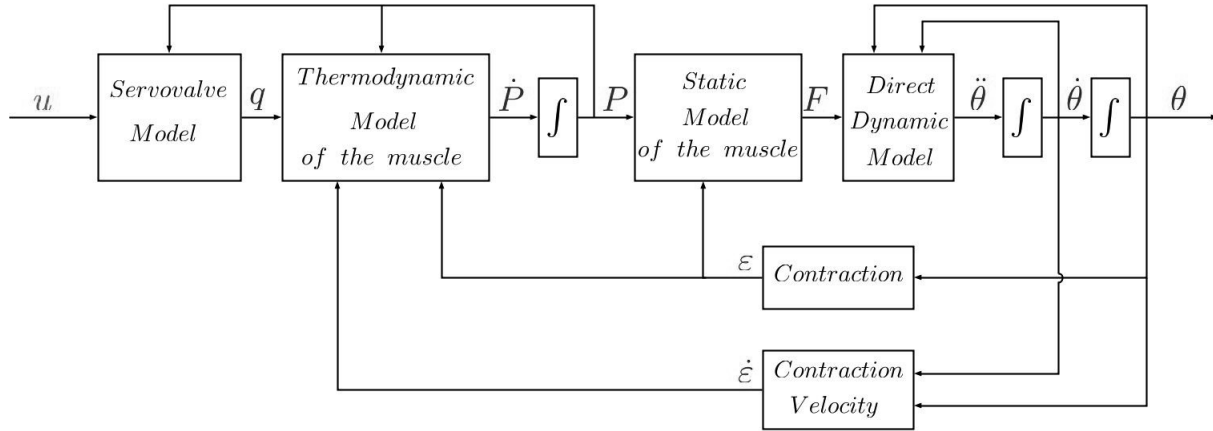


**FIGURE 7.** SIMULINK MODEL REPRESENTATION

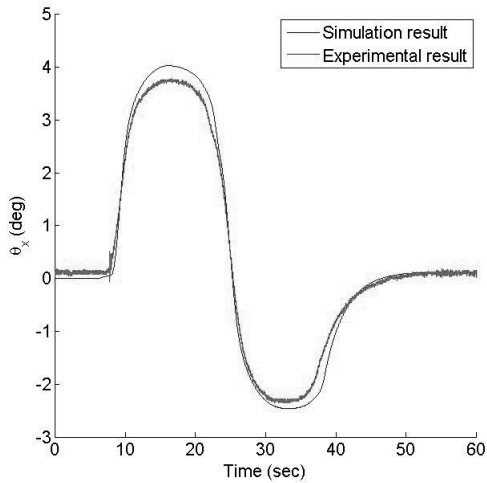


**FIGURE 8.** SIMULATION AND EXPERIMENTAL RESPONSE OF  $\theta_x$  FOR A RAMP INPUT IN  $u_1$  FOLLOWED BY A RAMP INPUT IN  $u_2$

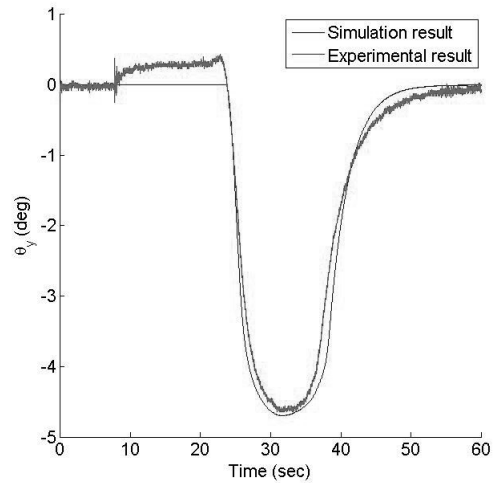


**FIGURE 9.** SIMULATION AND EXPERIMENTAL RESPONSE OF  $\theta_y$  FOR A RAMP INPUT IN  $u_1$  FOLLOWED BY A RAMP INPUT IN  $u_2$

the second muscle. Taking into account unmodeled uncertainties (like the friction), we can confirm, regarding the small errors observed between the simulation and experimental results that the model shows a good agreement with reality.

### INVERSE MODEL CONTROL

Once the model validated, a model based control synthesis can be defined. As we can see, our system is highly non linear, and thus non linear control strategies shall be called for stabilization, regulation or trajectory generation. One of these strategies

is the input-output linearization based on inverse model. Interestingly, this approach can be robust as far as the system is well modeled, because it strongly relies on the matching of the control model with the system's behavior. We proved that the system is invertible, but the proof will not be detailed in this article, neither some of the mathematical and analytic derivations. In the sequel, we will represent the final expressions of the inverse model control that allow us to generate the required voltage supply to the servovalve as function of the desired trajectory of the platform  $(\theta_x, \theta_y)$  and their successive derivatives. We proceed as follows: a resolution of the over-actuation is addressed. Then, having the

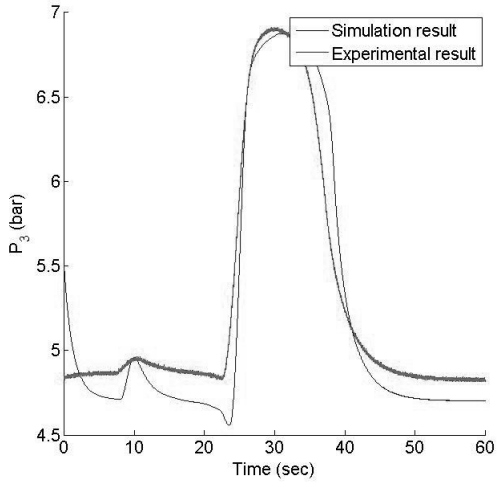


**FIGURE 10.** SIMULATION AND EXPERIMENTAL RESPONSE OF  $P_3$  FOR A RAMP INPUT IN  $u_1$  FOLLOWED BY A RAMP INPUT IN  $u_2$

desired trajectory and all needed derivatives, each model is analytically inverted, starting from the dynamic model of the platform, then the quasi-static and dynamic model of the muscle, to finally reach the servovalve model. This provides an expression of the required voltage inputs. The representation of the control is illustrated in Fig. 11.

### Over-Actuation Resolution

The system is clearly over-actuated, since three inputs are generated, and only two outputs are being controlled. The over-actuation can be remarked in eq. (17), where the effort  $F_3^d$  has to be arbitrarily chosen in order to calculate the other desired efforts  $F_1^d$  and  $F_2^d$ . Therefore, an allocation strategy is addressed by choosing  $F_3^d$  that makes the muscles perform at a certain range of desired pressure, and thus regulating the open-loop compliance of the system (we will also skip the details of resolution in this article). The method consists of calculating the minimum and the maximum allowed effort of the muscles at each static position ( $\theta_x$  and  $\theta_y$ ) of the platform, and then impose a desired value of the real time efforts exerted by the muscles by controlling a parameter  $\lambda$  such that:

$$F_3 = \lambda F_{max} + (1 - \lambda) F_{min}, \quad \lambda \in [0, 1]. \quad (16)$$

Thus, the choice of  $F_3$  at each position via the factor  $\lambda$  will affect the range of operation of the pressure in the muscle by eq. (6) as well as the desired efforts in the two other muscles, these efforts being calculated from eq. (17).

As example, in Fig. 12, two values of  $\lambda$  (0.65 and 0.5) are taken in two different tests for comparison. We can see that as  $\lambda$  increases, the operating range of the pressure  $P_3$  increases and vice-versa.

### Control Synthesis

We will denote by the superscript ( $d$ ) the desired variable that will be calculated in order to get the inputs. The desired efforts exerted by the muscles to the platform are found from the inverse dynamic model, that can be written as:

$$\begin{bmatrix} F_1^d \\ F_2^d \end{bmatrix} = E^{-1} \left( \theta_x^d, \theta_y^d \right) \left[ \begin{bmatrix} \ddot{\theta}_x^d \\ \ddot{\theta}_y^d \end{bmatrix} - G \left( \theta_x^d, \theta_y^d \right) F_3^d + \frac{1}{J} \Gamma_f \left( \dot{\theta}_x^d, \dot{\theta}_y^d \right) \right] \quad (17)$$

where the matrices  $E$  and  $G$  are given in eq. (18).

The desired pressures inside the muscles are obtained by inverting the quasi-static model of the muscle (eq. 6)

$$P_{gi}^d = \frac{F_i^d - L(\varepsilon_i^d)}{H(\varepsilon_i^d)}, \quad i = 1 \dots 3. \quad (19)$$

And by differentiating the quasi-static model of the muscle (eq. 6) w.r.t. time, we can explicit the expression of  $\dot{P}_i^d$  as:

$$\dot{P}_i^d = \frac{\dot{F}_i^d - \frac{\partial H(\varepsilon_i^d)}{\partial \varepsilon_i} \dot{\varepsilon}_i^d P_{gi}^d - \frac{\partial L(\varepsilon_i^d)}{\partial \varepsilon_i} \dot{\varepsilon}_i^d}{H(\varepsilon_i^d)}, \quad i = 1 \dots 3 \quad (20)$$

Equation (20) is used to calculate the desired flow from equation (15) by inverting the dynamic model of the muscle:

$$q_i^d = \frac{V(\varepsilon_i^d)}{krT} \dot{P}_i^d + \frac{P_i^d}{rT} \frac{\partial V(\varepsilon_i^d)}{\partial \varepsilon_i} \dot{\varepsilon}_i^d, \quad i = 1 \dots 3 \quad (21)$$

Note that  $\varepsilon_i^d$ ,  $\dot{\varepsilon}_i^d$  and  $V(\varepsilon_i^d)$  can be directly calculated from eq. (2), (3) and (9) respectively,  $\dot{F}_i^d$  is obtained by differentiating eq. (17) w.r.t. time.

The last step is to inverse the characteristics of the servovalve. Thus, a look-up table, that gives the desired voltage input  $u^d$  as function of the mass flow  $q^d$  and desired pressure  $P^d$  is constructed for each servovalve.

Figures 13 and 14 show two experimental results for a sine wave of amplitude  $5^\circ$  for  $\theta_x$  and  $2^\circ$  for  $\theta_y$ .

We can easily remark a phase difference between the desired signal and the output. Let us not forget that the inverse model control generates the open-loop inputs required for a desired trajectory. To overcome the uncertainties of the model, a PID controller controlling the desired angles is added as a feedback loop.

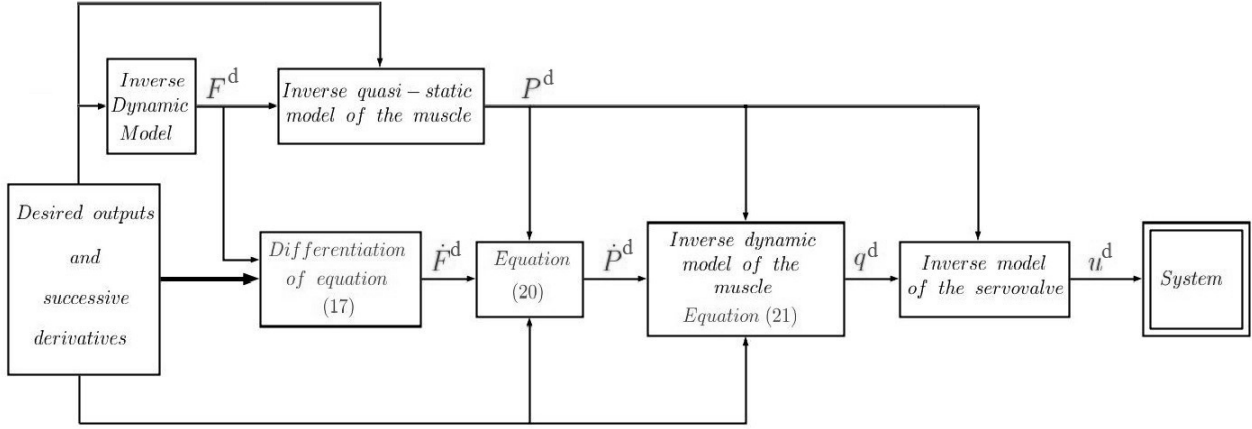


**FIGURE 11. INVERSE MODEL CONTROL**

$$\begin{cases} E(\theta_x, \theta_y) = \frac{R}{J} \begin{bmatrix} -\sin \phi_1 \cos \theta_x \cos \theta_y & -\sin \phi_2 \cos \theta_x \cos \theta_y \\ \cos \phi_1 \cos \theta_y + \sin \phi_1 \sin \theta_x \sin \theta_y & \cos \phi_2 \cos \theta_y + \sin \phi_2 \sin \theta_x \sin \theta_y \end{bmatrix} \\ G(\theta_x, \theta_y) = \frac{R}{J} \begin{bmatrix} -\sin \phi_3 \cos \theta_x \cos \theta_y \\ \cos \phi_3 \cos \theta_y + \sin \phi_3 \sin \theta_x \sin \theta_y \end{bmatrix} \end{cases} \quad (18)$$

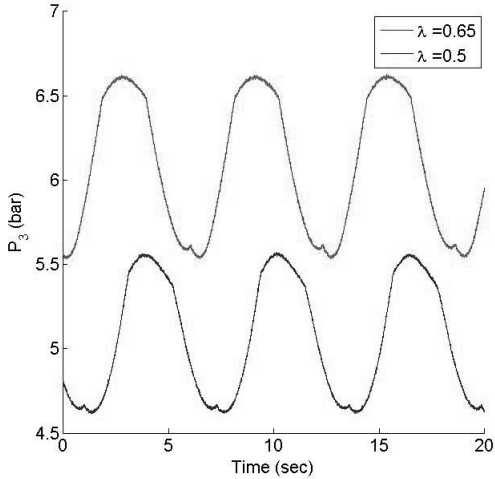


**FIGURE 12. OPERATING RANGE OF  $P_3$  WITH TWO DIFFERENT VALUES OF  $\lambda$**

The results of adding a PID regulator to the inverse model are shown in Fig. 15 and 16, where a desired trajectory, at least three times differentiable, is given for  $\theta_y$  and a sine wave trajectory is given to  $\theta_x$  in another test. A circular movement of the platform ( $\theta_y$  function of  $\theta_x$ ) is illustrated in Fig. 17 comparing the desired trajectory and the experimental one.

We can still observe an error of  $0.2^\circ$  at the peak points of the sine trajectory in Fig. 16.

## CONCLUSION

In this paper, a complete model of an horizontal platform actuated by three pneumatic artificial muscles has been derived. The validity of the complete model has been shown, and an inverse model control combined with a PID regulator has been applied to the system. Experimental results showed the efficiency of this control approach and an improved performance over a pure PID controller in the dynamic operating range. As perspective, we propose to consider other non linear model based control, combining inverse model with sliding mode control for

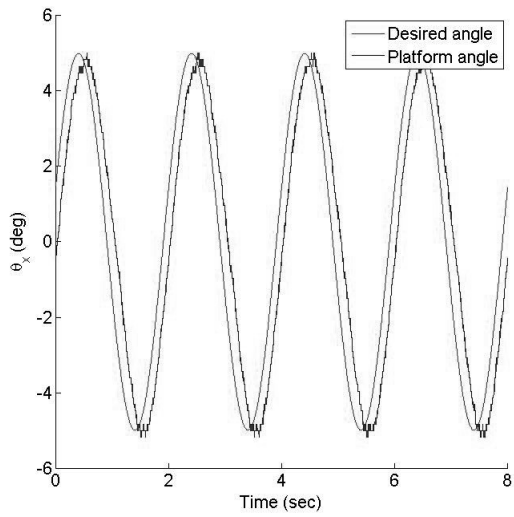


**FIGURE 13.**  $\theta_x$  ANGLE RESPONSE FOR A SINE WAVE TRAJECTORY WITH INVERSE MODEL CONTROL

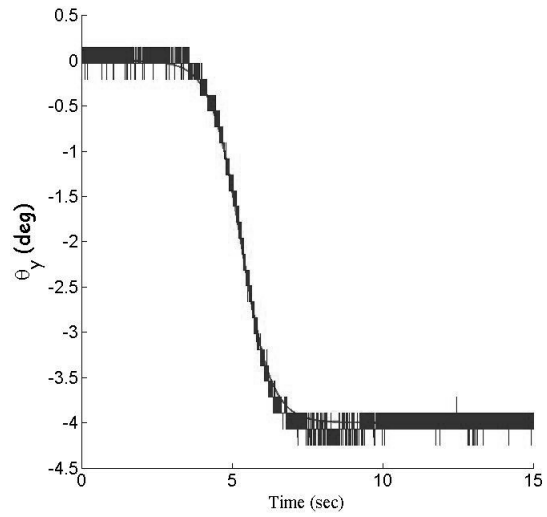


**FIGURE 15.**  $\theta_y$  ANGLE RESPONSE FOR A SMOOTH STEP TRAJECTORY WITH INVERSE MODEL CONTROL AND PID REGULATOR

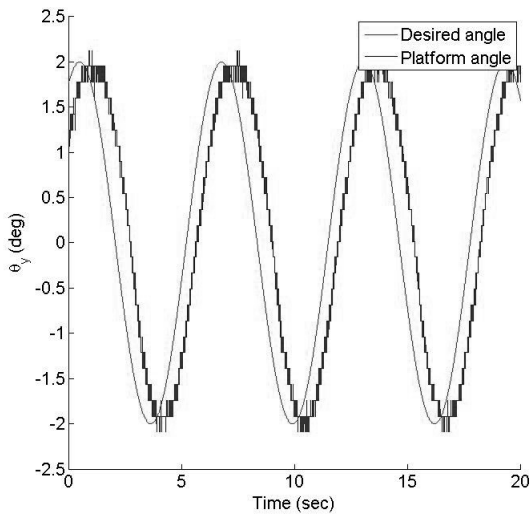


**FIGURE 14.**  $\theta_y$  ANGLE RESPONSE FOR A SINE WAVE TRAJECTORY WITH INVERSE MODEL CONTROL

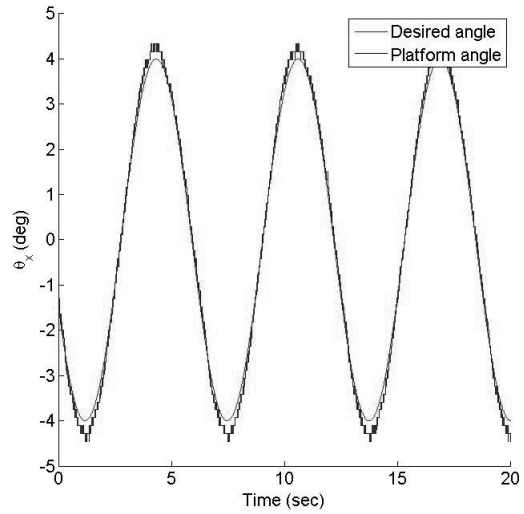


**FIGURE 16.**  $\theta_x$  ANGLE RESPONSE FOR A SINE WAVE TRAJECTORY WITH INVERSE MODEL CONTROL AND PID REGULATOR

example. A further step is to apply the strategy adopted in this paper for a Stewart platform based on six pneumatic muscles and having six degrees of freedom.

**REFERENCES**

[1] E. Bideaux, S. Sermeno Mena, S. S., 2012. "Parallel manipulator driven by pneumatic muscles". *8th International Conference on Fluid Power (8th IFK), Dresden, Germany.*  
 [2] Shi, G., and Shen, W., 2013. "Hybrid control of a parallel

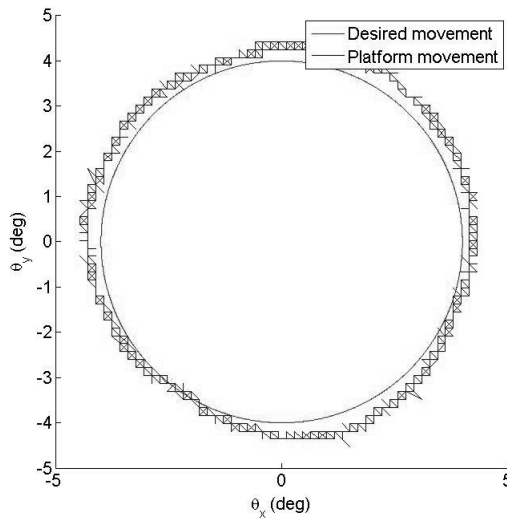


**FIGURE 17.**  $\theta_x$  CIRCULAR MOVEMENT OF THE PLATFORM FOR A SINE WAVE TRAJECTORY WITH INVERSE MODEL CONTROL AND PID REGULATOR

platform based on pneumatic artificial muscles combining sliding mode controller and adaptive fuzzy cmac”. *Control Engineering Practice*, **1**(1), pp. 76–86.

- [3] Goldstein, H., 1980. Classical mechanics.
- [4] Daerden, F., and Lefeber, D., 2002. “Pneumatic artificial muscles: actuators for robotics and automation”. *European journal of mechanical and environmental engineering*, **47**(1), pp. 11–21.
- [5] Chou, C.-P., and Hannaford, B., 1996. “Measurement and modeling of mckibben pneumatic artificial muscles”. *Robotics and Automation, IEEE Transactions on*, **12**(1), pp. 90–102.
- [6] Tondu, B., and Lopez, P., 2000. “Modeling and control of mckibben artificial muscle robot actuators”. *Control Systems, IEEE*, **20**(2), pp. 15–38.
- [7] Kang, B.-S., Kothera, C. S., Woods, B. K., and Wereley, N. M., 2009. “Dynamic modeling of mckibben pneumatic artificial muscles for antagonistic actuation”. In *Robotics and Automation, 2009. ICRA'09. IEEE International Conference on*, IEEE, pp. 182–187.
- [8] Olaby, O., Brun, X., Sesmat, S., Redarce, T., and Bidaux, E., 2005. “Characterization and modeling of a proportional valve for control synthesis”. In *Proceedings of the JFPS International Symposium on Fluid Power, Vol. 2005*, The Japan Fluid Power System Society, pp. 771–776.